Proceedings of Global Power and Propulsion Society
ISSN-Nr: 2504-4400
Beijing Conference 2019
16th – 18th September, 2019
www.gpps.global

GPPS-BJ-2019-0114

ACTIVE CONTROL OF THERMOACOUSTIC OSCILLATION USING MICROSECOND PLASMA DISCHARGE

Mingxuan Zhang
+86 15510918350
zmx951130@163.com
Beijing, China

Jingxuan Li
+86 18810950035
jingxuanli@buaa.edu.cn
Beijing, China

Wenwang Cheng
+86 13810900962
zhonghangda521@163.com
Beijing, China

Ting Li *
+86 18600883290
li1329@buaa.edu.cn
Beijing, China

1. **Beihang University**
2. **National Key Laboratory of Science and Technology Aero-Engine Aero-Thermodynamics**

ABSTRACT

As a thermoacoustic phenomenon that is widely appear in combustion devices, thermoacoustic oscillation can drive or adversely affect the system. Active control of the thermoacoustic oscillations with actuators helps to control it in the desired direction, commonly used actuators include speakers, jets, fuel spray etc. Different from the conventional actuators, the microsecond plasma discharge has the characteristics of small size and large sound pressure. Its acoustic characteristic allow it to generate specific pressure wave during discharge, thereby controlling thermoacoustic oscillations, and thus can be used as a novel control method. In this paper, the Rijke tube is used as a model to derive formula under normal temperature and pressure, and time domain simulation is carried out in Simulink tool to find the appropriate active control scheme. Finally, the experiment was carried out, and the wire mesh in the Rijke tube was heated by an electromagnetic induction device to generate thermoacoustic oscillation without punching holes on the tube. Then based on the waveforms of simulation results, the high-voltage microsecond discharge is used for closed-loop control on the thermoacoustic oscillation and significantly suppressed the oscillation.

KEY WORDS: THERMOACOUSTIC OSCILLATION, PLASMA, ACTIVE CONTROL

INTRODUCTION

Thermoacoustic instability is widespread in various types of combustion devices, its essence refers to the coupling of unsteady heat release and pressure disturbance, which causes the system to produce unstable oscillations and emit a sharp sound under certain conditions (Dowling, 2005). In the aero-engine combustion chamber, the oscillating sound pressure caused by the thermoacoustic instability can even reach about 10% of the average pressure, resulting in engine fatigue damage, reducing the service life of the equipment, and even causing accidental flameout or equipment damage. Therefore, it is necessary to simulate and control the thermoacoustic oscillation.

The most common control method for thermoacoustic oscillation is active closed-loop control (Zhao Dan, 2018), which refers to the use of speakers, jets and other actuators to change the flow field conditions to achieve control effects. However, traditional controllers often have defects such as large size and small adjustable range. For example, the sound pressure generated by the speaker is generally only a few tens of Pascals, and the control range that can be used is limited. So it is necessary to consider new actuators to achieve better control effects. In recent years, plasma discharge has been applied to control thermoacoustic instability in the case of flame heat sources. Due to the plasma assisted combustion, the plasma generated by the discharge at the flame can effectively stabilize the flame in the central region, suppress the combustion instability, and reduce the amplitude of the generated sound pressure (Jonas, 2013; Kim, 2015). The corresponding experiments were applied to the Rijke tube and the swirl burner, which proved its effectiveness as an actuator for thermoacoustic instability control. However, there is still a lack of application of plasma discharge to control the thermoacoustic instability of non-flame heat sources by plasma assisted combustion. The acoustic characteristic of plasma allow it generate specific

pressure wave during discharge, a high-voltage pulsed plasma power source that uses a pin-to- pin electrode can generate a specific pressure wave and has a small size and a large sound pressure, and it is very feasible to consider it as a new actuator for thermoacoustic oscillation control of non-flame heat sources.

As the most classical and simple experimental device for studying thermoacoustic oscillations, the Rijke tube has been used repeatedly by researchers as a model sichance its birth (Morgans, 2007). The common Rijke tube is a glass tube or a metal tube, and a wire mesh is placed in the lower half to be heated to produce thermoacoustic oscillation. The purpose of this paper is to use the Rijke tube as a model, perform time domain simulation in Simulink tool, and find the appropriate control scheme. After that, the plasma discharge power source was used as an actuator to conduct experiments. According to the simulation result, the phase difference between the power trigger signal and the thermoacoustic oscillating pressure wave is adjusted, the electrode spacing is also accurately set to control the discharge pressure amplitude to an appropriate value, and finally a good control effect is obtained.

MATHEMATICAL DESCRIPTION OF MODEL

In this paper, the Rijke tube with open ends is used as a model. It is assumed that the axial length of the heat source is extremely short, and the tube is divided into two regions, upstream and downstream. The intensity of the incident wave in the upstream and downstream is m and f, respectively, and the intensity of the reflected wave is k and g (Mcintosh, 1996). The sound pressure sensor is installed downstream of the tube, the actuator is a plasma discharge device, it is installed at the upstream entrance of the tube. The overall arrangement is as shown in Fig. 1.

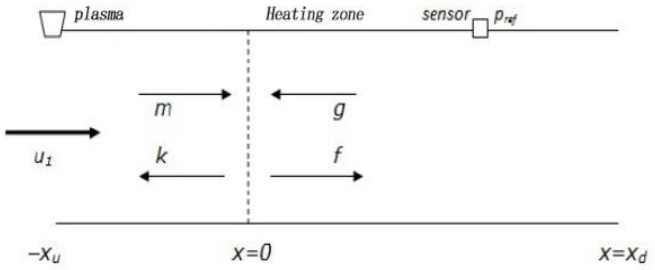

Figure 1 Overall Layout of Rijke Tube

It is assumed that the pressure, velocity and density of the upstream and downstream regions follow the linear wave equation. Based on the intensity of the incident and reflected waves, the upstream parameter can be expressed as:

$$p(x,t)=\bar{p}_1+k(t+\frac{x}{\bar{c}_1-\bar{u}_1})+m(t-\frac{x}{\bar{c}_1+\bar{u}_1}) \quad (1)$$

$$u(x,t)=\bar{u}_1+\frac{1}{\bar{\rho}_1\bar{c}_1}(m(t-\frac{x}{\bar{c}_1+\bar{u}_1}) -k(t+\frac{x}{\bar{c}_1+\bar{u}_1})) \quad (2)$$

$$\rho(x,t)=\bar{\rho}_1+\frac{1}{\bar{c}_1^2}(m(t-\frac{x}{\bar{c}_1+\bar{u}_1}) +k(t+\frac{x}{\bar{c}_1-\bar{u}_1})) \quad (3)$$

Similarly, downstream parameters can also be expressed in the same form. At the upstream and downstream boundaries, the reflection will cause loss of wave intensity and will bring a certain time delay. Here, the boundary conditions are given:

$$m(t)=R_u k(t-\frac{2x_u}{\bar{c}_1(1-M_1^2)})+i(t-\frac{x_u}{\bar{c}_1+\bar{u}_1}) \quad (4)$$

$$g(t)=R_d f(t-\frac{2x_d}{\bar{c}_2(1-M_2^2)}) \quad (5)$$

One-dimensional form of the N-S equation (mass, momentum and energy equation) in the Rijke tube is introduced:

$$[\rho u]_1^2=0 \quad (6)$$

$$[p+\rho u^2]_1^2=0 \quad (7)$$

$$[(c_pT+0.5)\rho uA]_1^2=Q \quad (8)$$

There equations are integrated to obtain the equation at the heat source, the expression of instantaneous heat release can be obtained by the relationship between the upstream and downstream parameters, the step equations at the heat source are:

$$(p_2-p_1)+\rho_1u_1(u_2-u_1)=0 \quad (9)$$

$$\frac{\gamma}{\gamma-1}(p_2u_2-p_1u_1)+\frac{1}{2}\rho_1u_1(u_2^2-u_1^2)=\frac{Q}{A} \quad (10)$$

Where γ is the ratio of specific heat and Q is the heat release. The expressions of pressure, velocity and density are then brought in to obtain the strength calculation equation and written in the form of a matrix. The main basis of the simulation is to solve the equation (Dowling, 1995).

$$\begin{pmatrix}X_{11} & X_{12}\\ X_{21} & X_{22}\end{pmatrix}\begin{pmatrix}f(t)\\ k(t)\end{pmatrix}=\begin{pmatrix}Y_{11} & Y_{12}\\ Y_{21} & Y_{22}\end{pmatrix} \begin{pmatrix}f(t-\tau_d)R_d\\ k(t-\tau_u)R_u\end{pmatrix}+\begin{pmatrix}C_{11}\\ C_{21}\end{pmatrix}i(t-\frac{X_u}{\bar{u}_1+\bar{c}_1}) +\begin{pmatrix}0\\ 1\end{pmatrix}\frac{Q'(t)}{A\bar{c}_1} \quad (11)$$

Where,

$$X_{11}=1+M_1\frac{\bar{\rho}_1\bar{c}_1}{\bar{\rho}_2\bar{c}_2},\ X_{12}=-1+M_1(2-\frac{\bar{u}_2}{\bar{u}_1})-M_1^2(1-\frac{\bar{u}_2}{\bar{u}_1})$$

$$X_{21}=\frac{\bar{c}_2}{\bar{c}_1}\frac{1+\gamma M_2}{\gamma-1}+M_1M_2\frac{\bar{\rho}_1}{\bar{\rho}_2},$$

$$X_{22}=\frac{1-\gamma M_1}{\gamma-1}+M_1^2-M_1^2(1-M_1)\frac{1}{2}(\frac{\bar{u}_2^2}{\bar{u}_1^2}-1)$$

$$Y_{11}=M_1\frac{\bar{\rho}_1\bar{c}_1}{\bar{\rho}_2\bar{c}_2}-1, Y_{12}=1+M_1(2-\frac{\bar{u}_2}{\bar{u}_1})+M_1^2(1-\frac{\bar{u}_2}{\bar{u}_1})$$

$$Y_{21}=\frac{\bar{c}_2}{\bar{c}_1}\frac{1-\gamma M_2}{\gamma-1}+M_1M_2\frac{\bar{\rho}_1}{\bar{\rho}_2},$$

$$Y_{22}=\frac{1+\gamma M_1}{\gamma-1}+M_1^2-M_1^2(1+M_1)\frac{1}{2}(\frac{\bar{u}_2^2}{\bar{u}_1^2}-1)$$

$$C_{11}=1+M_1(2-\frac{\bar{u}_2}{\bar{u}_1})+M_1^2(1-\frac{\bar{u}_2}{\bar{u}_1})$$

$$C_{21}=\frac{1+\gamma M_1}{\gamma-1}+M_1^2-M_1^2(1+M_1)\frac{1}{2}(\frac{\bar{u}_2^2}{\bar{u}_1^2}-1)$$

In order to solve the strength equation, the combustion model must be properly selected, this paper selects a simple $n-\tau$ model (Zhao Dan, 2014; Gelbert, 2012). However, since the frequency of unstable oscillations in the Rijke tube is generally first-order or second-order, the combustion model should pay more attention to the low-order frequency, so a low-pass filter is added to the $n-\tau$ model. It should be noted that the above combustion model is still a linear model. The actual saturation process of oscillation is due to nonlinearity (Balasubramanian, 2008), so nonlinear factors must be introduced into the model to stimulate the limit cycle oscillation. Therefore, the model (Li, 2015) is used to introduce nonlinear parameters between heat release perturbations and velocity perturbations. The relationship between the nonlinear flame transfer function G and the linear flame transfer function T can be expressed as:

$$G(\frac{u'}{\bar{u}},s)=f*T(\frac{u'}{\bar{u}}) \tag{12}$$

While f describes the saturation of heat release rate with velocity perturbations, and f can be determined according to the following formula:

$$\frac{q'(\frac{u'}{\bar{u}},0)}{\bar{q}}=f*\frac{u'}{\bar{u}}=\int_0^{u'/\bar{u}}\frac{1}{1+(\xi+\alpha)^\beta}d\zeta \tag{13}$$

α and β are two coefficients which determine the shape of the nonlinear model. There is a saturation limit $(u'/\bar{u})^s$ during the thermoacoustic instability oscillation. For weak velocity disturbances, the link between $(q'/\bar{q})$ and $(u'/\bar{u})$ is linear, but when the disturbances exceeds saturation limit, f decreases and the heat release rate perturbations begin to saturate. The parameter α determines the level of saturation limit, $(u'/\bar{u})^s$ decreases as α increases toward unity. As for the parameter β, it controls the smoothness of the saturation corner. The smaller the parameter β, the smoother the saturation corner. In this paper, $\alpha=0.85, \beta=30$, which is in line with the actual oscillation amplitude, and the simulation oscillation waveform corner is quite smooth. Integrate the above formula into Matlab software for time domain simulation in Simulink module

TIME DOMAIN SIMULATION AND CONTROL SCHEME

Import the formula deduced in the previous section into Matlab software, and set the normal temperature and pressure parameters according to the actual experimental conditions. The boundary conditions at both ends of the Rijke tube are also being selected.

Working Condition Parameters			
M_1	0.01	T_1	$293.15K$
T_2	$550K$	ρ_1	$1.2041kg/m^3$
P_1	$101325Pa$	τ_1	$0.01s$
τ_f	$0.001s$	n_f	5
R_u	-0.95	R_d	-0.95

Table 1 Working Condition Parameters Consistent with Experimental Conditions

The combustion and acoustic models are built in the Simulink tool, and the thermoacoustic oscillation time domain simulation is performed, the result is shown in Figure 2. The measurement frequency of the instability is 203 Hz, and the saturation amplitude is close to 140 Pa.

In order to achieve the best control effect in the experiment, it is necessary to find the most appropriate control strategy under this condition. The overall idea of the control scheme is to use the sensor to detect the amplitude and phase of the thermoacoustic oscillation sound pressure, and then use the controller to set the amplitude and phase of signal, finally output the signal through the actuator to form a closed loop feedback control (Hathout, 1998; Heckl, 1986; Gulati, 1992). In this paper, the phase shift control method is adopted, and the filter is used for feedback control.

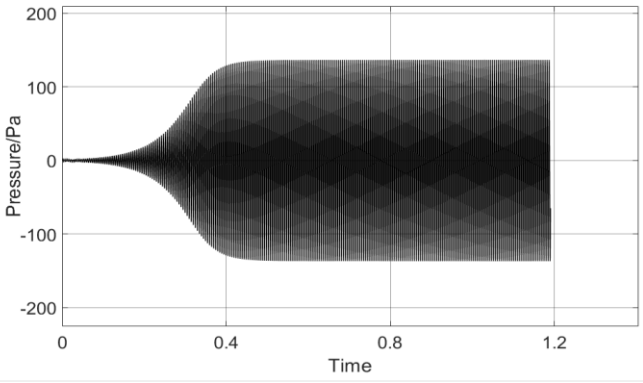

Figure 2 Thermoacoustic Oscillation Time Domain Simulation

The unstable frequency of thermoacoustic oscillation is mainly low-order, but in order to suppress the instability caused by high-order frequencies, it is necessary to introduce a filter. This paper uses a second-order low-pass filter, the form is as follows:

$$G(s)=\frac{\omega^2}{s^2+2\kappa\omega s+\omega^2} \tag{14}$$

The frequency of the first-order oscillation in the time domain simulation is $1275rad/s$. In order to suppress the high-order frequency instability, the value of ω in the filter expression is increased, taking $\omega=2000,\kappa=0.5$.

The controller that is used to suppress the instabilities is phase shift compensator with the high voltage pulse discharge device used to add feedback control. In order to achieve good control effects, a second-order phase shift controller is used here. The structure of the active controller is of the form (Annaswamy, 1998):

$$K(s)=\frac{K(s-a)^2}{(s+a)^2} \tag{15}$$

In the formula, the unit of a is Hz, and the second-order unstable frequency is used, so taking $a=435$ .Then determine the value of K according to the actual control effect and the Nyquist criterion to get the best control effect, and finally determine $K=0.2$.

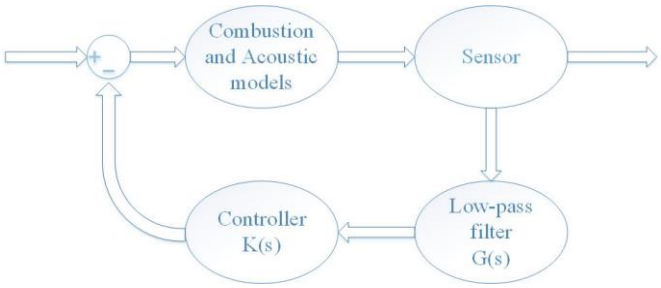

Figure 3 Control Strategy Flow Chart

After obtaining the control scheme, feedback control is performed in the Simulink tool, and good control effect is obtained. After 1.2s, the amplitude of the thermoacoustic oscillation tends to be zero. Based on this, the same strategy as the control scheme is adopted in the experiment to make a fixed phase difference between the plasma discharge signal and the thermoacoustic oscillation pressure, and the discharge pressure amplitude is appropriately set to complete the entire control.

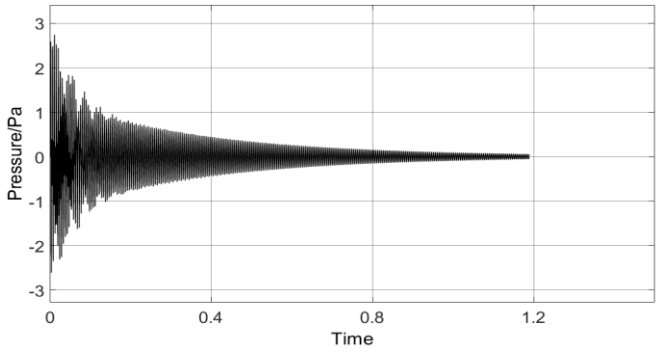

Figure 4 Thermoacoustic Oscillation Controlled by Phase Shift Method

EXPERIMENTAL SETUP

After the simulation is completed, the experiment is carried out under the working condition of normal temperature and pressure. Firstly, a vertical glass tube with length of 1 m and an inner diameter of 54mm is supported by an aluminum alloy bracket built on an optical table, then a stainless steel piece is supported by three ceramic rods with a diameter of 3mm at a length of 1/4 of the tube from the lower end of the tube. The diameter of the ceramic rod is extremely small, so the influence on the flow field is negligible (Matveev, 2003). The stainless steel piece is heated by an electromagnetic induction heat source (HAIRUITUO HTG-3AC), thermoacoustic oscillation occurs when the heating power reaches a certain value (Matveev, 2004).

Then, the sound pressure in the tube is measured by the sensor (BSWA MPA401) and data is transmitted to data acquisition card (NI PCI-6221) by the BNC connector (BNC-2090A). The phase is adjusted by the Labview software according to simulation. The output signal is translated to the high-voltage microsecond pulse power source (CAS High Voltage Microsecond Pulse Power Supply), and plasma is generated by the pin-to-pin electrode discharge. During the discharge procedure, a specific sound wave is generated, which is called the acoustic characteristic of the plasma. The spacing between the pin-to-pin electrodes is directly related to the amplitude of the generated acoustic waves (Sutton, 2011) the larger the spacing, the larger the amplitude of the acoustic waves, so the control effect can be achieved by adjusting the distance between the electrodes.

Figure 5 Overall Test Bench

After measuring the frequency and amplitude of the thermoacoustic oscillation sound wave in the tube, it is necessary to set the trigger signal frequency of the high voltage power supply to be consistent with the oscillation sound wave. The distance between the electrodes is then adjusted to obtain a discharge acoustic amplitude that is consistent with the simulation results. Finally, the phase difference between the trigger signal and the oscillating sound wave is constantly changed to form a closed-loop control to achieve the final control effect.

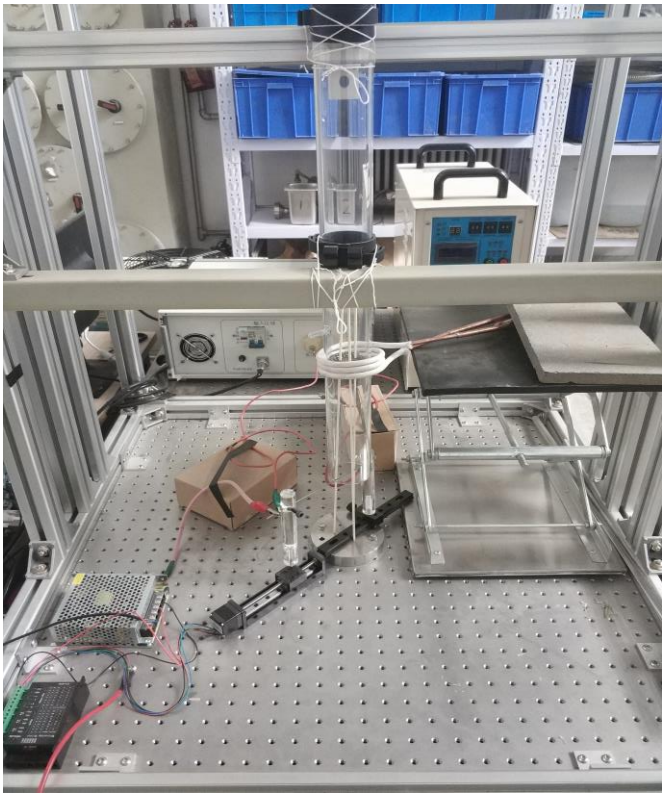

Figure 6 Rijke Tube Detail

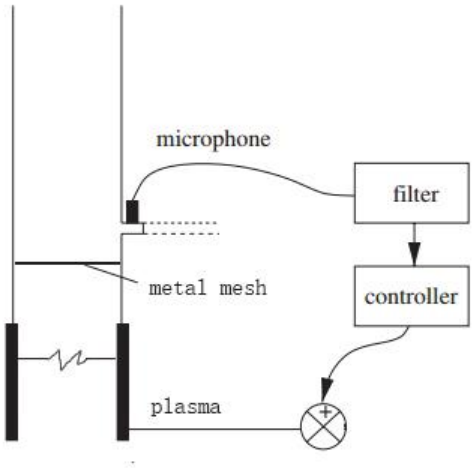

Figure 7 Experimental Flow Chart

PROCEDURE AND RESULT

In order to confirm the discharge sound pressure property, firstly, the acoustic wave in the tube generated by discharge alone was measured. The high-voltage microsecond pulse power supply is internally composed of an insulated gate bipolar transistor (IGBT). Due to the special nature of the IGBT, the pulse width of the pulse discharge signal is fixed at 8 microseconds. The power supply is connected to the pin-to-pin electrode, and the voltage of the power supply capacitor is continuously increased until the discharge voltage of the electrode can penetrate the air to generate plasma. The pulse width of the trigger signal adapted to the pulse power supply is 6-30 microseconds. First of all, the trigger signal was set to a pulse with a frequency of 100 Hz and a pulse width of 20 microseconds, and the discharge result was measured for the pin-to-pin electrode. Fig. 8 is a graph showing the discharge sound pressure when the distance of electrode is 5 mm and the frequency is 100 Hz. It can be observed that the sound pressure waveform is relatively stable and the amplitude is large, indicating that the plasma discharge control range is large. It is worth mentioning that sound pressure amplitude is changed by adjusting the electrode spacing to further control the thermoacoustic oscillation.

A prerequisite for control is to excite the thermoacoustic oscillations inside the tube. The experiment was carried out under normal temperature and normal pressure condition, and the stainless steel piece was supported in the tube at a length of 25cm from the lower end of the tube, and it was heated by an electromagnetic induction heating device to cause thermoacoustic oscillation in the tube. When the heating power reached 1.5kW, the thermoacoustic oscillation in the tube was excited. Then the amplitude and phase of the thermoacoustic oscillation was monitored with the sensor installed on the upper part of the tube at a distance of 25cm from top of this tube, and it passed to the acquisition card by the BNC connector. As shown in Fig. 9, the thermoacoustic oscillation frequency at the initial moment is 230 Hz, and the amplitude is about 140 Pa, which is in good agreement with the simulation results although the frequency is slightly higher than simulation result.

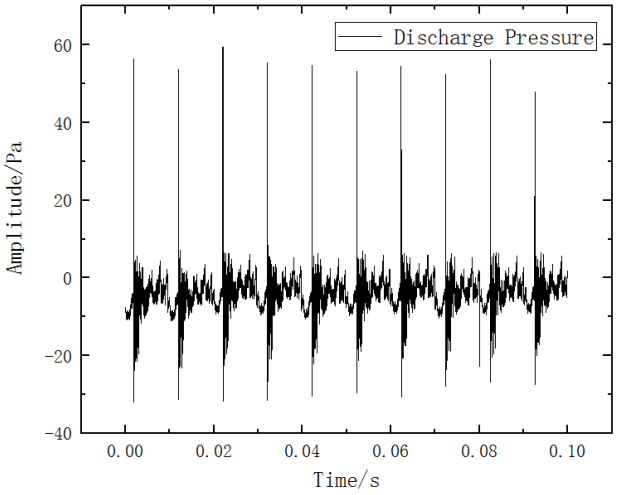

Figure 8 Discharge Waveform with Electrode Spacing of 5 mm and Frequency of 100 Hz

Then, the trigger signal of the high-voltage pulse power source was adjusted to a frequency consistent with the sound pressure of the thermoacoustic oscillation, therefore, the trigger signal had a frequency of 230 Hz and the pulse width was set to 20 microseconds. In order to avoid frequent corrosion of the electrodes, a 1.6 mm diameter tungsten needle was used for discharge. The distance of electrode was continuously adjusted so that the discharge sound pressure was 20% of the amplitude of sound pressure in the tube according to the simulation. At this time, the distance

between the double-needle electrodes was 3.5 mm, and the voltage for generating plasma by breaking down air was about 11.8 kV. Finally the phase difference between the discharge pulse was adjusted, and good control effect was achieved.

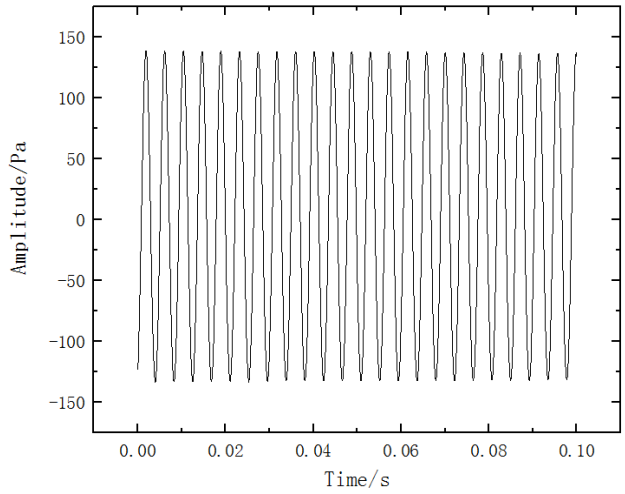

Figure 9 Initial Sound Pressure of Thermoacoustic Oscillation in the Tube

Fig. 10 shows the oscillation waveform within 0.1 s after discharge control, it can be seen that the average pressure amplitude is reduced to about 30 Pa. In the frequency domain diagram of the sound pressure level of Fig. 11, it is reflected that the first-order unstable sound pressure level is reduced by about 12 dB, indicating that effective control is obtained by plasma discharge control. In addition, the discharge will cause a certain fluctuation of the thermoacoustic oscillation pressure, so the amplitude of controlled pressure wave will have a small range of fluctuations during the entire control process, which is also reflected in Figure 10 and 11.

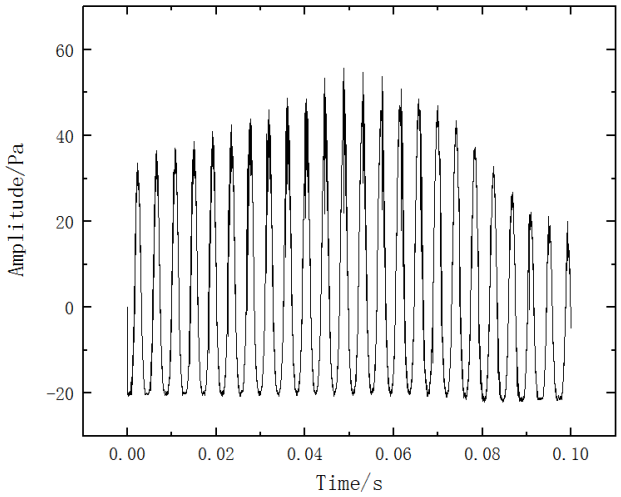

Figure 10 Control Waveform after Continuous Discharge

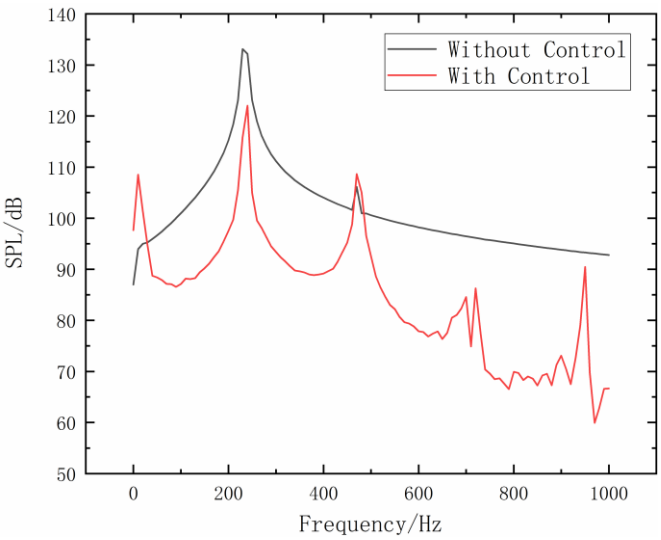

Figure 11 The Effect of control on the pressure spectrum

Conclusion

The strength calculation equation of thermoacoustic oscillation is derived by using Rijke tube as a model under normal temperature and pressure. Assuming that the pressure, velocity, and density parameters follow linear wave equation, the final calculated intensity equation matrix is obtained using the transition equation at the heat source. And the $n-\tau$ model with first-order low-pass filter is selected for time-domain simulation of thermoacoustic oscillation, nonlinear parameter is also introduced to ensure nonlinear saturation simulation. The phase shift method and second-order low-pass filter is used for closed-loop control, the amplitude and phase of the feedback acoustic wave signal are adjusted to obtain a good control effect.

Using the acoustic characteristic of the plasma, a specific pressure wave can be generated during the discharge process, and a high-voltage microsecond discharge generator is used with continuous discharge by pin-to-pin electrodes. According to the simulation results, the phase of the discharge signal and the distance between electrodes are adjusted, the distance is adjusted to control the discharge pressure amplitude as 11% of the thermoacoustic oscillation amplitude. Finally, the sound pressure level of the thermoacoustic oscillation is reduced by about 12 dB after continuous discharge control, and a certain active control effect is obtained.

The above conclusions show that plasma discharge has a good control effect on thermoacoustic oscillation, and it has the advantages of small size and large adjustable range as a closed-loop controlled actuator, which is a very promising way to do the active control of the thermoacoustic oscillation.

ACKNOWLEDGMENTS

This work was supported by NSFC 51606005, National Key Laboratory of Science and Technology Aero-Engine Aero-Thermodynamics and Beihang University.

References

Dowling A P, and Morgans A S. (2005). Feedback control of combustion oscillations. Annual review of fluid mechanics 37 (1), 151-182. doi:10.1115/GT2015-42126

Zhao D, Lu Z, and Zhao H. (2018). A review of active control approaches in stabilizing combustion systems in aerospace industry. Progress in Aerospace Sciences doi:10.1016/j.paerosci.2018.01.002

Morgans A S, and Dowling A P. (2007). Model-based control of combustion instabilities. Journal of Sound and Vibration 299 (1-2) 261-282. doi:10.1016/j.combustflame.2007.06.002

Mcintosh A C, and Rylands S. (1996). A model of heat transfer in Rijke tube burners. Combustion Science & Technology 113(1) 273-289.

Dowling A P. (1995). The calculation of thermoacoustic oscillations. Journal of Sound and Vibration 180(4) 557-581. doi:10.1006/jsvi.1995.0100

Zhao D, and Reyhanoglu M. (2014). Feedback control of acoustic disturbance transient growth in triggering thermoacoustic instability. Journal of Sound and Vibration, 333 (16) 3639-3656. doi:10.1016/j.jsv.2014.04.015

Gelbert G, Moeck J P, and Paschereit C O. (2012). Feedback control of unstable thermoacoustic modes in an annular Rijke tube. Control Engineering Practice 20(8). doi:10.1016/j.conengprac.2012.03.016

Balasubramanian K, and Sujith R I. (2008). Thermoacoustic instability in a Rijke tube: Non-normality and nonlinearity. Physics of fluids, 20 (4). doi:10.1063/1.2895634

Li J, and Morgans A S. (2015). Time domain simulations of nonlinear thermoacoustic behaviour in a simple combustor using a wave-based approach. Journal of Sound and Vibration 346 345-360. doi:10.1016/j.jsv.2015.01.032

Hathout J P, Annaswamy A M, and Fleifil M. (1998). A model-based active control design for thermoacoustic Instability. Combustion Science and Technology 132 (1-6) 99-138. doi:10.1080/00102209808952012

Heckl M A. (1986). Active control of the noise from a rijke tube. Aero- and Hydro-Acoustics. Springer Berlin Heidelberg. doi: 10.1007/978-3-642-82758-7_18

Gulati A, and Mani R. (1992). Active control of unsteady combustion-induced oscillations. Journal of Propulsion and Power 8(5) 1109-1115. doi: 10.2514/3.23599

Annaswamy A M, El Rifai O M, and Fleifil M. (1998). A model-based self-tuning controller for thermoacoustic instability. Combustion Science and Technology, 135 (1-6) 213-240. doi:10.1080/00102209808924158

Matveev K I , and Culick F E C. (2003). A study of the transition to instability in a Rijke tube with axial temperature gradient. Journal of Sound and Vibration, 264(3) 689-706. doi:10.1016/s0022-460x(02)01217-8

Matveev K I. (2004). Energy consideration of the nonlinear effects in a Rijke tube. Journal of Fluids & Structures 18(6) 783-794. doi: 10.1016/j.jfluidstructs.2003.07.016.

Sutton Y. (2011). Electro-acoustic coupling in a plasma gas. PhD thesis, Open University.

Jonas P. Moeck. (2013) Control of combustion dynamics in a swirl-stabilized combustor with nanosecond repetitively pulsed discharges. 51st AIAA Aerospace Science Meeting including the New Horizons Forum and Aerospace Exposition. doi:10.2514/6.2013-565

Kim W, Snyder J, and Cohen J. (2015) Plasma assisted combustor dynamics control. Proceedings of the Combustion Institute, 35 (3) 3479-3486. doi:10.1016/j.proci.2014.08.025